CHAPTER 54

WAVE DIRECTION MEASUREMENT USING MARINE X BAND RADAR

Hiromaru Hirakuchi, Masaaki Ikeno

ABSTRACT

Spatial radar signals received by a conventional marine radar are digitized as a 8-bit word by means of an A/D converter. The numerical procedure is discussed to estimate the two-dimensional radar spectrum from a digitized radar image. Directional spectra of sea waves are also observed by a 3-component wave array. A comparison of the mean wave direction and period estimated from the radar spectrum with the results from the array spectrum shows that the developed data acquisition system and numerical procedure represent a reliable and very cost-effective means to observe the properties of sea waves.

1. INTRODUCTION

In addition to wave height and period, wave direction has great influence upon the coastal problems. The measuring techniques for wave direction can be classified into two major groups, the direct measurement method and the remote sensing method. In recent years, considerable interest has been showed in the application of the remote sensing techniques; a synthetic aperture radar (SAR) mounted on a satellite or an airplane, a shore-based high frequency (HF) radar. One of such studies has dealt with the use of a marine X band radar.

Ijima et.al.(1964) and Wright(1965) were the first to report the use of the marine radar for imaging ocean waves. Willis and Beaumont(1971), Evmenov et.al.(1973), and Mattie and Harris(1978) have also presented photographic radar images. In order to estimate the mean wave direction and period, these early researchers visually inspected the radar images as displayed on the plane position indicator (PPI).

Making use of the digitized radar images, Hoogeboom and Rosenthal(1982) and Young et.al.(1985) have calculated the 2- and 3-dimensional spectra of the spatial radar images. It appears that the numerical procedure is very useful to determine the properties of ocean waves. In these studies, however, the radar images displayed on the PPI were once recorded on photographic films, and the

Senior Research Engineer, Central Research Institute of Electric Power Industry, Abiko, Abiko-Shi, Chiba, Japan.

photographic images were digitized by means of an image processor. Therefore, it is difficult to apply a marine radar to routine data collection.

The purpose of this study is to overcome some of the technical difficulties associated with the routine data collection and to verify the numerical procedure employed for analysis of digitized radar images through comparison with the directional wave spectra obtained by the direct measurement method.

2. MARINE RADAR SYSTEM

The marine X band radar used in this study is of the conventional rotating type. Parameters of the radar system are as follows: frequency of 9.4GHz, antenna type of 2.81m slotted wave guide, nominal peak power of 25kW, pulse length of 20ns at 5.6km range, pulse repetition frequency of 2000Hz, antenna rotation speed of 24rpm, HH polarization, and horizontal/vertical beam width of 0.8°/25°.

The data acquisition system is shown schematically in Fig.1. The intensity of the reflected signals from nearby sea surface is stronger than that from distant sea surface. In order to extend the measurable range of distance, the received signals were fed into a log-amplifier, and the resultant signals were digitized as a 8-bit word (0-255) by means of an A/D converter controlled by a personal computer. The digitized images were stored on floppy disks.

Two successive radar images, having time delay of the antenna rotation period, can be observed by the system. Each radar image in a quadrant area with the angle of 90° consists of 256 pixels along a radar beam and 512 pixels along an arc. The sampling frequency along a radar beam is 10MHz; the distance resolution and range are 15m and 3.84km, respectively. The azimuthal signals of the rotating antenna are used to collect the proper azimuthal data; The azimuthal resolution is about 0.176°.

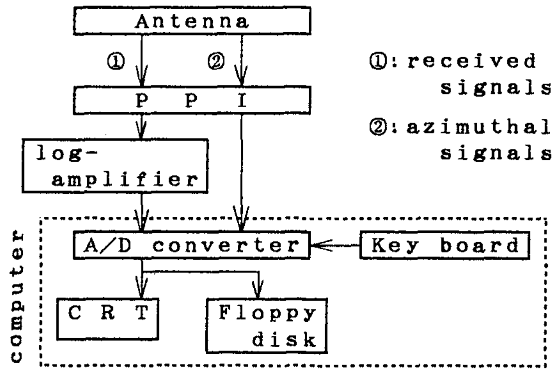

Fig.1 Flow diagram of data acquisition system.

3. FIELD OBSERVATION

A field observation was carried out near the coast of Kashiwazaki, Japan, in Feb., 1988. The marine radar was mounted on a rooftop at the distance of 50m from the shoreline: the height of the antenna is about 20m above the sea level. Fig.2 shows the observation area. Four radar images each with a different direction were observed every 2 hours during two periods; from 18:00 on 15 to 12:00 on 17, and from 16:00 on 27 to 12:00 on 29. As shown in Fig.2, the direction of the first radar image is from 200° to 290°, second 220°-310°, third 245°-335°, and forth 290°-20°. Where the direction is defined clockwise from the north.

In addition to the radar system, five wave arrays were also deployed to observed the directional spectra of sea waves, as shown in Fig.2, where ST.1-ST.5 represent the wave observation points. ST.1 and ST.4 are 10m deep, ST.3 and ST.5 are 20m deep, and ST.2 is 15m deep. A 3-component wave array was used for the direct wave measurement; a supersonic wave gauge and a two-component electro-magnetic current meter. The wind speed and direction during this observation were measured by Tokyo Electric Power Company at the point A and B in Fig.2. The heights of A and B are 10m and 78m from the grand level, respectively; 20m and 160m from the sea surface, respectively.

An example of the digitized radar images of the 3rd quadrant (245°-335°) are shown in Fig.3(a)-(c), which were observed at 6:00 on Feb. 16 (CASE-1), at 0:00 on Feb. 17 (CASE-2), and at 20:00 on Feb. 27 (CASE-3). Incident wave directions in Fig.3(a) and Fig.3(c) are about 290° and 0°, respectively. The striking feature in Fig.3(b) is the pronounced bi-directional sea state.

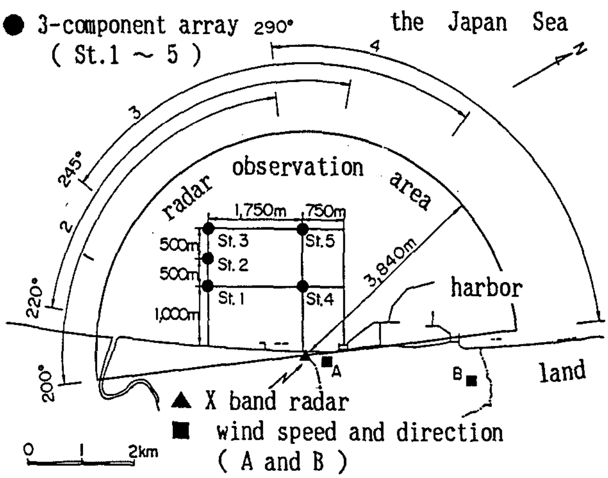

Fig.2 Field observation area.

In this study, radar images for CASE-1, 2 and 3 are examined. Wind data at point A and wave data are shown in Table 1, together with the data observed before and after 2 hours of each radar observation.

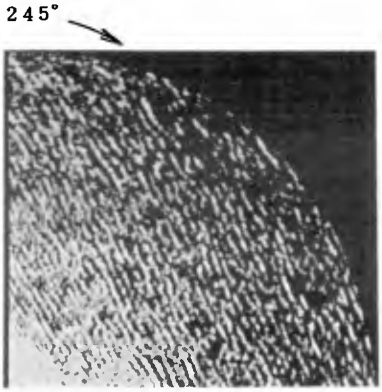

(a) CASE-1 (at 6:00 on Feb. 16)

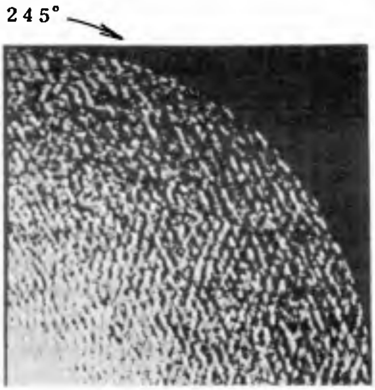

(b) CASE-2 (at 0:00 on Feb. 17)

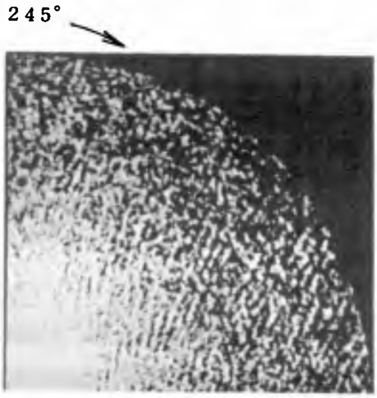

(c) CASE-3 (at 20:00 on Feb. 27)

Fig.3 Observed radar images.

4. DATA PROCESSING

4.1 DISTANCE CORRECTION

The intensity of the radiated energy decreases with the square of the distance from the antenna, and the intensity of the backscattered energy also decreases with the square of the distance from the target.

Table 1 Wind and wave data summary.

	Date & Time 1988 Feb.	Wind Speed & Direction (m/s)		Wave Height (cm) $\begin{bmatrix} H_{1/3} \\ 4\sqrt{m_0} \end{bmatrix}$					Wave Period $\begin{bmatrix} T_{1/3} \text{ (sec)} \\ f_p \text{ (Hz)} \end{bmatrix}$					Wave Direction (deg) $\begin{bmatrix} \theta M \\ \theta 0 \end{bmatrix}$			
				ST.1	ST.2	ST.3	ST.4	ST.5	ST.1	ST.2	ST.3	ST.4	ST.5	ST.1	ST.2	ST.3	ST.4
①	16,	15.3	NNW	---	213	253	215	213	----	6.32	6.31	6.33	6.37	---	327	340	322
	4:00			---	231	259	224	227	----	0.115	0.125	0.129	0.168	---	318	322	316
	16,	15.7	NNW	268	273	309	276	263	7.34	7.15	7.04	6.82	7.03	322	320	320	323
	6:00			280	283	313	279	275	0.125	0.133	0.121	0.111	0.123	320	316	314	312
	16,	16.8	NNW	279	269	263	254	254	7.38	7.10	6.89	7.15	6.79	318	322	323	325
	8:00			296	284	276	259	273	0.119	0.117	0.119	0.145	0.115	318	318	320	316
②	16,	12.6	NNW	190	178	216	184	183	7.15	6.79	6.68	6.26	6.27	321	322	330	322
	22:00			205	189	231	199	219	0.119	0.117	0.127	0.182	0.193	324	312	326	318
	17,	11.9	NNW	180	170	181	183	174	6.73	6.06	6.83	7.11	6.98	322	319	326	324
	00:00			189	178	194	193	199	0.109	0.111	0.107	0.107	0.104	328	318	322	320
	17,	8.4	NNW	161	157	157	153	157	7.33	6.89	6.75	6.71	7.49	321	325	322	322
	2:00			174	174	168	169	189	0.117	0.109	0.111	0.113	0.109	330	336	322	318
③	27,	9.2	NW	79	90	91	86	91	4.60	5.16	4.69	4.75	4.99	360	350	339	342
	18:00			90	102	102	96	98	0.260	0.125	0.258	0.133	0.260	330	2	4	348
	27,	9.0	NW	101	94	112	106	119	4.58	5.01	4.93	4.77	4.85	331	334	330	335
	20:00			112	103	121	113	124	0.109	0.107	0.223	0.115	0.238	330	4	350	338
	27,	12.9	NW	130	135	119	129	116	4.79	4.87	4.89	5.01	4.83	322	327	335	326
	22:00			137	142	128	138	126	0.195	0.201	0.123	0.197	0.203	326	326	352	316

H1/3, T1/3 : significant wave height and period defined by zero-crossing method.
$4\sqrt{m_0}$: representative wave height estimated from 0th moment (m_0) of wave power spectrum.
fp : peak frequency of wave power spectrum.
θm : mean wave direction calculated from 1st moment of directional spectrum.
θ0 : peak direction of integrated directional spreading function.
①, ②, ③ : CASE-1, 2 and 3

However, the clutter cross-section is proportional to the distance from the antenna, because the depression angle of the antenna is very small. Therefore, the intensity of the received signals varies inversely as a cube of the distance, rather than inversely as the fourth power as is the case for point targets. In the radar system, the received signals were fed into a log-amplifier, so that the digitized radar signals are expressed as follows:

$$\zeta = \log C = \log \lambda + \log \sigma_o - 3 \log R \qquad \text{----(1)}$$

where ζ is the signal through the log-amplifier, C is the received signal, σ_o is the cross section per unit area, R is the distance from the antenna, and λ is defined as

$$\lambda = P_t G A_e \theta_B (c\tau / 2) / (4\pi)^2 \qquad \text{---(2)}$$

Where P_t is the transmitter power, G is the antenna gain, A_e is the antenna effective aperture, θ_B is the azimuthal beam width, c is the velocity of radar propagation, and τ is the radar pulse width.

log λ in Eq.(1) is a constant value, because λ is associated with the only specifications of the radar antenna as shown in Eq.(2). Since the distance range considered in this study is from 1 to 4km offshore, log R in Eq.(1) is approximated to a linear line over this range. log σ_o in Eq.(1) represents the intensity of sea clutter, so that its spatial variation is very important to estimate the wave direction and period.

If the characteristics of the sea surface are spatially homogeneous, a spatially averaged value of log σ_o is in close proximity to a constant value. On these assumptions, the signals after correcting the distance effect along a radar beam were expressed as follows:

$$\xi = \zeta - \delta(R), \qquad \delta(R) = a + bR \qquad \text{---(3)}$$

where ξ is the distance corrected signal, $\delta(R)$ is the fitting line, a and b are coefficients of a least square approximation.

Examples of the digitized radar signals along a radar beam are shown in Fig.4. Fig.4(a) represents the typical signals reflected from the wind wave surface. The signals in the range of 1km are saturated owing to the strong echo. However, the signals over that range show the images of the irregular sea waves. The fluctuated curve around 0 level indicates the signals after distance correction which was carried out over the range of 1km. This figure shows the property of the distance correction method described above.

Fig.4(b) represents the signals observed under the snowy weather condition. Characteristics of this case are that intensity level is high, but the fluctuation of the signals is very small. It is difficult to recognize the wave image in Fig.4(b) owing to the radar scattering from snow.

Fig.4(c) was observed under the calm condition. Wind speed was less than 2m/s, and the significant wave height and period were about 1.2m and 8s, respectively. Swell can not be detected outside the breaker zone. This figure indicates that short ripples generated by the wind are essential to the detection of long waves.

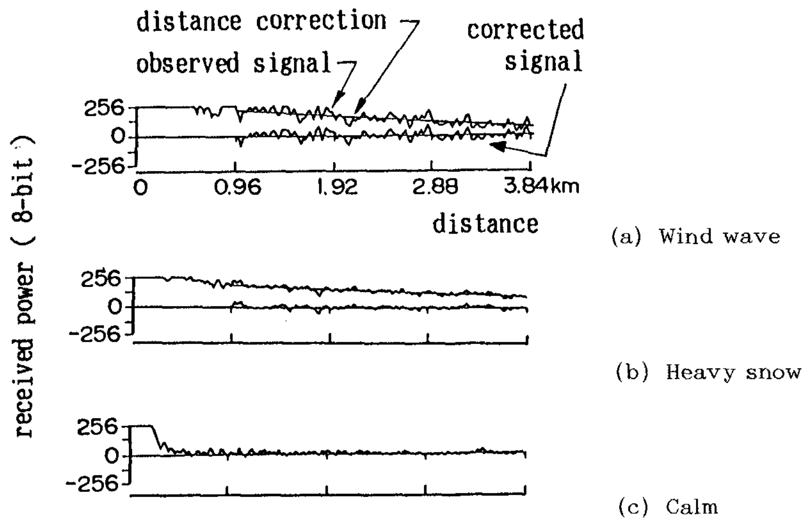

Fig.4 Example of digitized radar signals along a radar beam.

4.2 RADAR SPECTRAL ESTIMATION

The data analysis procedure is shown in Fig.5(a). After correcting the distance effect, the digitized radar image defined in the polar coordinate system is converted to the Cartesian coordinate system. A square region with a length of 960m as shown in Fig.5(b) is extracted from the converted data.

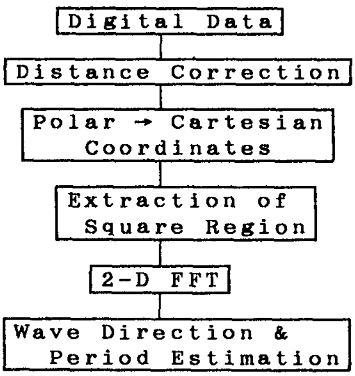

Fig.5(a) Data analysis procedure.

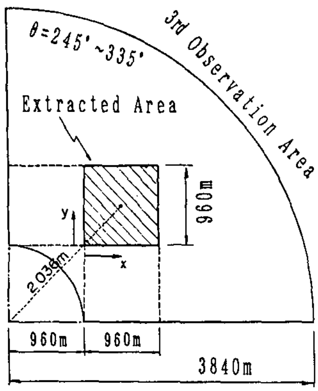

Fig.5(b) Analyzed area.

Fig.6 shows an example of the extracted spatial radar image and the wave number spectrum calculated from the 2D-FFT procedure. It is difficult to estimate the wave direction from Fig.6(b), because a 180° directional ambiguity exists in Fig.6(b) which has point symmetry. It is possible to remove this ambiguity by use of two successive images (Atanassov et.al.(1985)). However, this ambiguity can be removed by assuming that the reflected waves from the beach are very weak and most of the waves are coming from the offshore. Using this assumption, mean wave direction and period can be estimated from the wave number at the radar spectral peak, making use of the dispersion relationship.

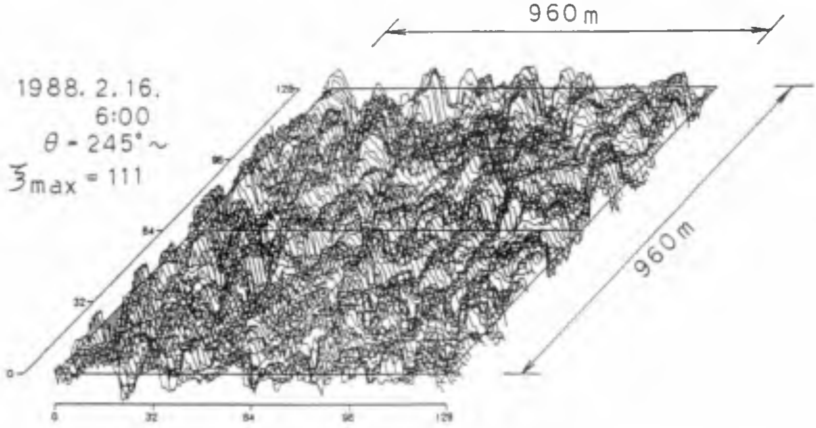

(a) Spatial radar image

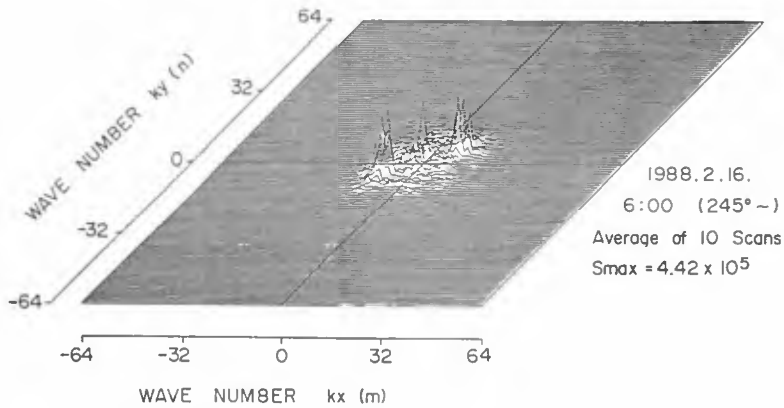

(b) Wave number spectrum

Fig.6 Example of spatial radar image and wave number spectrum.

5. RESULTS

Fig.7(a) for CASE-1 represents the wave numbers at the radar spectral peaks observed every five minutes from 5:50 to 6:10 on 16, together with the results of the averaged radar spectrum. ① and ② denote a first and second spectral peak, respectively. The wave numbers observed every five minutes represent slightly different values owing to the statistical variation of the random sea surface; the directional estimate from a radar image has a statistical error of about 10°. The averaged radar spectrum should be used to estimate the mean wave direction and frequency.

The wave direction and period estimated from the averaged radar spectrum were compared with those observed by the 3-component wave array. The contours in Fig.7(b) represent the directional wave spectrum observed at ST.3, making use of the extended maximum likelihood method (EMLM) proposed by Isobe et.al.(1984). As shown in Fig.7(b), the peak of the directional spectrum and integrated directional function represent the directions of 304° and 314°, respectively. The first peak of the radar spectrum is the direction of 313°, which is in good agreement with the array estimate.

Fig.8(a) for case-2 shows the results observed every five minutes from 23:50 on 16 to 0:10 on 17. Since the wave number ① and ② in Fig.8(a) are rather stable results in five radar spectra, the radar spectrum exhibits a bimodal directional distribution with the major peak at 341° and 313°, the frequency of 0.11Hz and 0.125Hz. However, the direction and period at the radar spectral peaks are much different from the results of the array spectrum, as shown in Fig.8(b).

The array spectrum observed 4 hours later than CASE-2 measurement are shown in Fig.9, together with the results of wave number ① and ② obtained in CASE-2. In Fig.9, the directions of the array spectrum which represents the bimodal structure show good agreement with ① and ②, although the frequencies of the array spectrum are slightly low. Fig.9 shows that the bimodal structure observed by the radar spectrum in Fig.8(b) is probably a true indication of the wave field.

Fig.10 for case-3 represents the results observed at 20:00 on 27. In this case, only one radar image is used for wave number estimation.
The array spectrum in Fig.10 observed at ST.3 represents the two distinct spectral peaks; the long and short waves with the frequency of 0.12Hz and 0.22Hz, respectively. The direction of the long waves is about 345°, which is in good agreement with the results of radar spectral peaks (346°). The wave direction of the long waves in CASE-3 is approximately 45° further to the north than that of CASE-1.

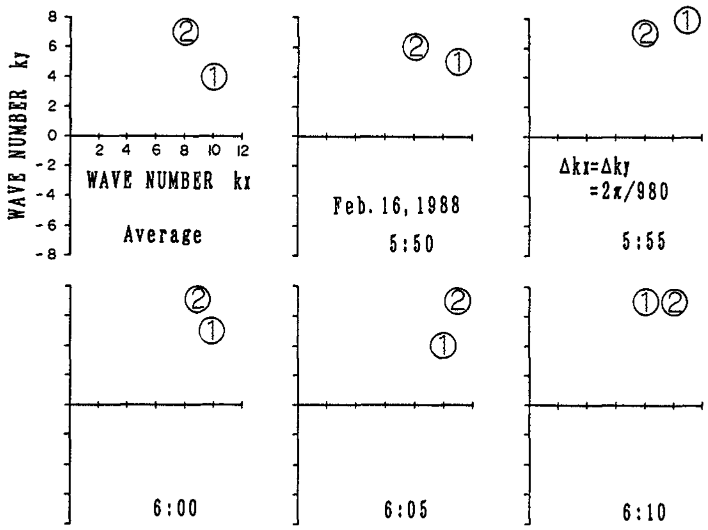

(a) Wave numbers at first and second peak of radar spectrum.

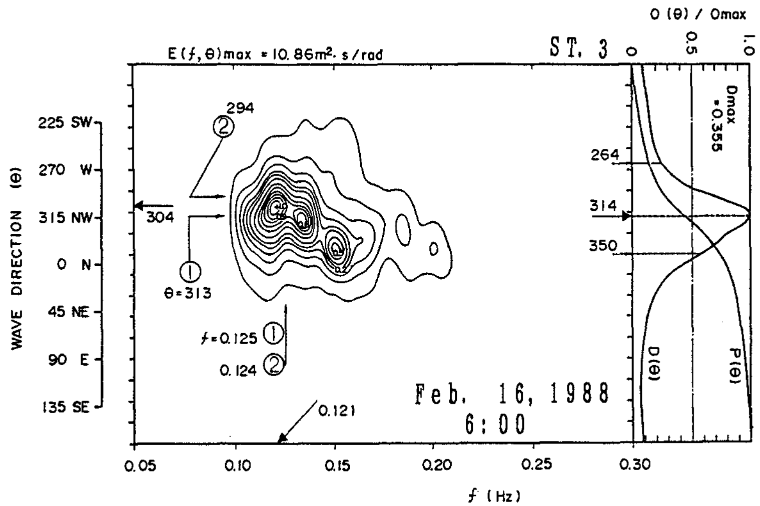

(b) Directional spectrum observed by wave array.

Fig.7 Comparison of wave direction and period for CASE-1.

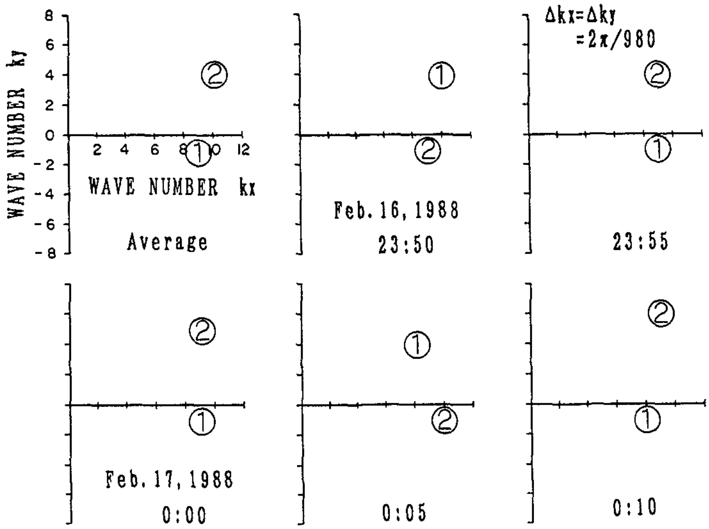

(a) Wave numbers at first and second peak of radar spectrum.

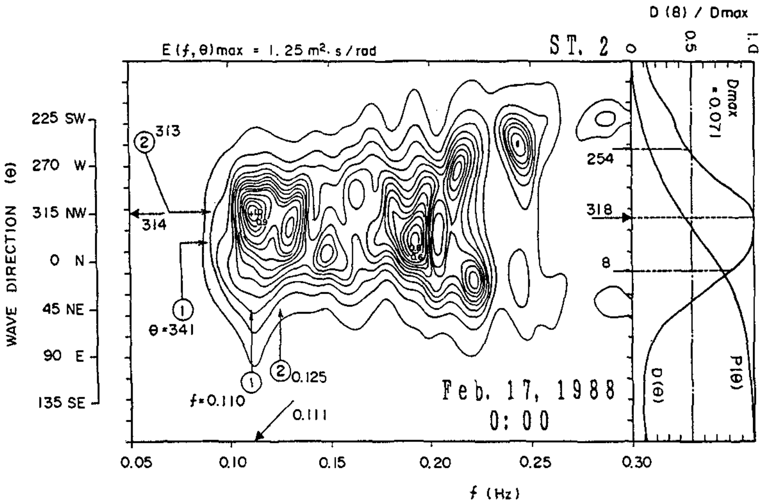

(b) Directional spectrum observed by wave array.

Fig.8 Comparison of wave direction and period for CASE-2.

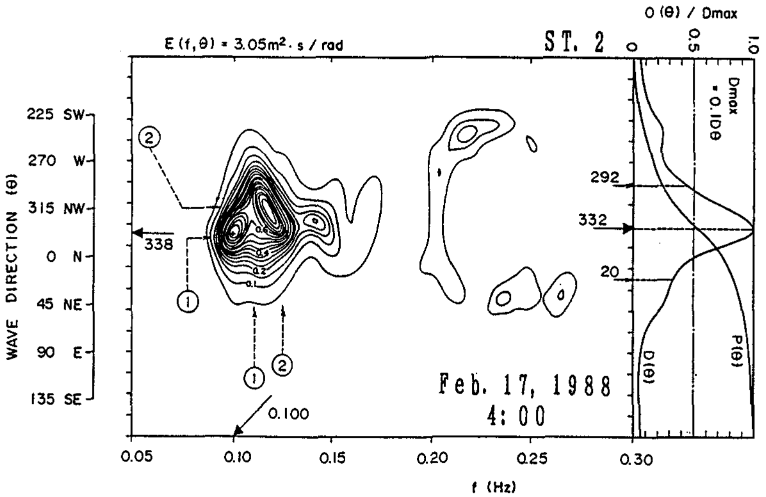

Fig.9 Directional spectrum observed 4 hours later than CASE-2.

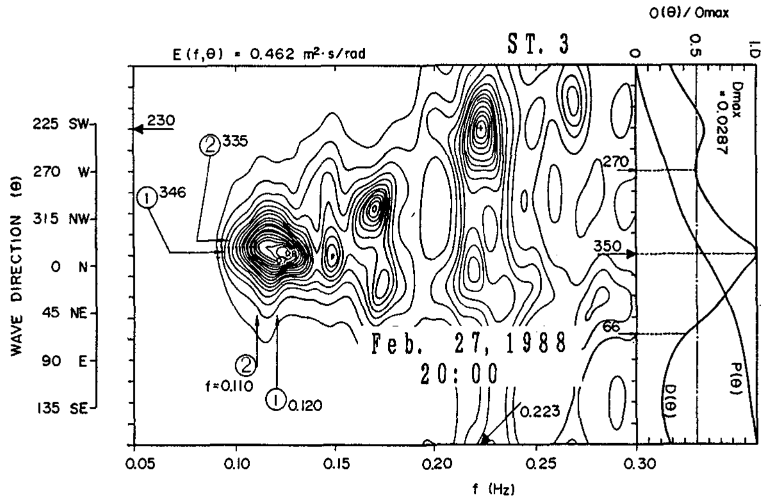

Fig.10 Comparison of wave direction and period for CASE-3.

6. CONCLUSIONS

The data acquisition system has been developed to record the spatial radar signals, and the numerical procedure employed for analysis of the digitized radar images has been proposed. Using this radar system and numerical procedure, the mean wave direction and period in the uni- and bi-modal wave field can be estimated more easily than the conventional method. Moreover, it will be possible to record the consecutive radar images by means of this system and to calculate the three-dimensional radar spectrum.

REFERENCES

Atanassov,V., W.Rosenthal, and F.Ziemer (1985) : Removal of ambiguity of two-dimensional power spectra obtained by processing ship radar images of ocean waves, J.G.R., Vol.90, No.C1, pp.1061-1067.

Ijima,T., T.Takahashi, and H.Sasaki (1964) : Application of radars to wave observations, Prod. of 11th Japanese Conf. of Coastal Eng., pp.81-88.(in Japanese)

Isobe,M., K.Kondo, and K.Horikawa (1984) : Extension of MLM for estimating directional wave spectrum, Proc. Symp. Description and Modelling of Directional Seas, Tech. Univ. Denmark, Paper No.A-6, pp.1-15.

Evmenov,V.F., I.V.Kozhukhov, N.T.Nichiporenko, and G.D.Khulop (1973) : Test of the radar method of defining ocean wave elements, Fluid Mechanics - Soviet Research, Vol.2, No.5, pp.141-145.

Hoogeboom, P., and W.Rosenthal(1982) : Directional wave spectra in radar images, International Geoscience and Remote Sensing Symposium, IEEE.

Mattie,M.G., and D.L.Harris (1978) : The use of imaging radar in studying ocean waves, Proc. of 16th Conf. on Coastal Eng., pp.174-189.

Willis,T.G. and H.Beaumont (1971) : Wave direction measurement using sea surveillance radars, Tech. Memo. TR 118, Royal Aircraft Establishment.

Wright,F.F. (1965) : Wave observation by shipboard radar, Ocean Sci. and Ocean Eng., Vol.1, pp.506-514.

Young, I.R., W.Rosenthal, and F.Ziemer (1985) : A three-dimensional analysis of marine radar images for the determination of ocean wave directionality and surface currents, J.G.R., Vol.90, No.C1, pp.1049-1059.